

Soft Measurement of Road Adhesion Coefficient Volumetric Kalman Filtering

Penghao Ji^{1, *}, Jiquan Wu¹

¹ School of Automotive and Transportation, Tianjin University of Technology and Education, Tianjin, China

* Corresponding author: Penghao Ji (Email: jipenghao0831@163.com)

Abstract: In order to solve the problem that the road adhesion coefficient is not extensive enough and difficult to obtain in practice, this paper designs a soft measurement method of road adhesion coefficient based on the volumetric Kalman filter theory. A three-degree-of-freedom vehicle estimation model using the Dugoff tyre model is established, and the validity and accuracy of the algorithm are verified with the help of the joint simulation platform of Carsim and Matlab/Simulink. The results show that the estimation error of the proposed estimation algorithm is within 5% under the three road adhesion coefficients, and the initial design can be completed well in terms of accuracy and real-time performance.

Keywords: Road adhesion coefficient, Kalman filter, Volumetric Kalman filter.

1. Introduction

The purpose of this paper is to develop a soft measurement algorithm for road surface adhesion coefficient estimation through experimental simulation, through which a higher computational accuracy and faster response speed can be achieved, which is conducive to further development and research in the automotive industry. Meanwhile, the real-time estimation of the road surface adhesion coefficient is an important part of the safety control of the vehicle, and is also a necessary prerequisite for the vehicle to carry out a series of stability control strategies. There are many methods and types of soft measurement of road surface adhesion coefficient in the present research, which can be divided into two categories of Cause-based and Effect-based according to different data acquisition and measurement methods[1]. The Cause-based approach applies past experience to estimate the current state of the road attachment coefficient, and generally applies conditions that have a large impact on the road attachment coefficient to the calculations and predictions[2]. For example: Optical sensors work by recognising water and other substances that reduce the coefficient of adhesion of the road surface, while Mika Morii and Hiroyuki Yasuo use a laser beam with a maximum power of 200W to illuminate the road surface for estimation[3]. Effect-based methods are carried out to analyze the response of the tyre or vehicle to estimate the road adhesion coefficient, tyre noise and tread deformation are mainly referred to collectively as the tyre response, and longitudinal dynamics and lateral dynamics are mainly referred to collectively as the vehicle response. Due to practical conditions, sensors are generally expensive and less robust, and easily affected by environmental factors, while the Cause-Based method requires additional sensors and is therefore not widely utilized. The Effect-Based method can accurately estimate road adhesion coefficients, and has the advantage of being more robust compared to the Cause-Based method. Cause-Based method has the advantages of being more robust and less expensive, but its computation is prone

to hysteresis, real-time is not high, and the amount of computation is generally large[4]. Therefore, Kalman filter and its many improved forms are being widely used in the study of vehicle driving state and vehicle parameter estimation, which is a relatively effective estimation method and estimation means. Among them, the theory of Extended Kalman Filter (EKF) must be used to expand the nonlinear system with Taylor's expansion formula to be linearised, otherwise it will lead to dispersion of the filter output data and non-convergence. Unscented Kalman Filter (UKF) has the advantage of high computational accuracy, but it is based on the standard Kalman filter, which is an infinite-growth memory filter, and when the filter estimation is performed at any moment, all the data prior to the current moment are used, leads to underutilized of current sensor measurements. Cubature Kalman filter (Cubature Kalman Filter) is derived from the Bayesian estimation of Gaussian function assumption, using the third-order spherical-radial volume criterion, the nonlinear system filtering into a Gaussian probability density function product of the integral solution of the problem, which has a rigorous mathematical proof of numerical integration through the third-order volume law approximates the weighted Gaussian integral. It has $2n$ volume points with equal weights (n is the number of system state dimensions), and it has been proved that its accuracy of approximating the probability distribution after the nonlinear transformation is better than that of the UKF, and it is simple to implement, and it has a high scalability, so it has a very broad application value[5].

2. Dynamical Model

2.1. Vehicle Model

Vehicle dynamic models can be used not only for vehicle motion and control, but also for tyre force calculation and road adhesion coefficient estimation. As shown in Fig. 1, this paper simplifies the vehicle into a 3-degree-of-freedom model with only three directions: longitudinal, lateral and transverse[6].

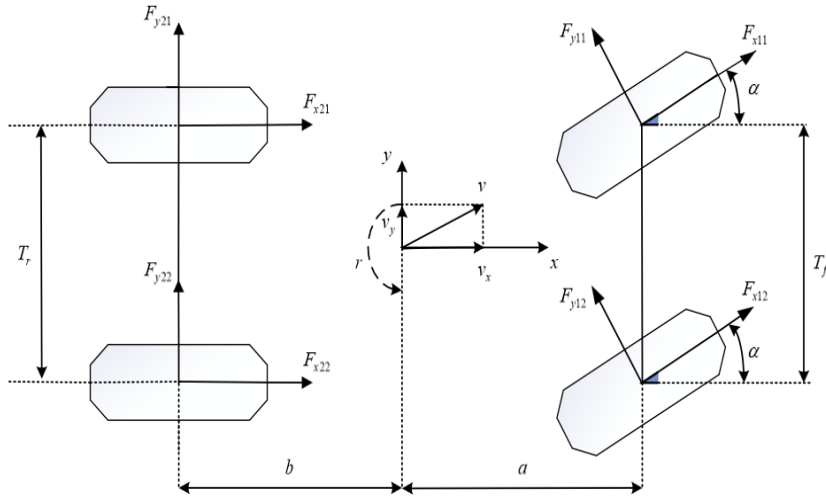


Figure 1. Vehicle dynamics modelling

The vehicle dynamics equations are:

$$\begin{cases} ma_x = (F_{x11} + F_{x12})\cos\alpha + F_{x21} + F_{x22} - (F_{y11} + F_{y12})\sin\alpha \\ ma_y = (F_{x11} + F_{x12})\sin\alpha + F_{y21} + F_{y22} + (F_{y11} + F_{y12})\cos\alpha \\ I_z \dot{\omega} = a(F_{x11} + F_{x12})\sin\alpha + a(F_{y11} + F_{y12})\cos\alpha - b(F_{y21} + F_{y22}) \\ \quad + \frac{T_f}{2}(F_{y11} - F_{y12})\sin\alpha - \frac{T_f}{2}(F_{x11} - F_{x12})\cos\alpha - \frac{T_r}{2}(F_{y21} - F_{y22}) \end{cases} \quad (1)$$

$$\begin{cases} F_{xij} = \mu F_{xij}^* = \mu F_{zij} C_{xij} \frac{s}{1-s} f(k) \\ F_{yij} = \mu F_{yij}^* = \mu F_{zij} C_{yij} \frac{\tan\alpha}{1-s} f(k) \end{cases} \quad (4)$$

In the above equation, a_x 、 a_y for the longitudinal acceleration and lateral acceleration of the vehicle; v_x 、 v_y for the longitudinal speed and lateral speed of the vehicle; a 、 b for the distance from the center of mass of the vehicle to the front and rear axes; m for the total mass of the vehicle; T_f 、 T_r for the distance between front and rear wheels; F_{xij} 、 F_{yij} for the longitudinal and lateral forces on the wheels ($i=1,2$ for the front axle and the rear axle, respectively, and $j=1,2,3,4$ for the left-front, right-front, left-rear, and right-rear wheels, respectively); α is the angle of gyration of the front wheels; I_z for the rotating moment of inertia; and $\dot{\omega}$ for the angular acceleration of the transverse swing.

2.2. Tyre Model

For the research content of this paper, considering the effect of model accuracy, Dugoff tyre model is selected, for each wheel, the longitudinal force and lateral force acting on the tyre can be expressed by equation (2).

$$\begin{cases} F_{xij} = \mu F_{zij} C_{xij} \frac{s}{1-s} f(k) \\ F_{yij} = \mu F_{zij} C_{yij} \frac{\tan\alpha}{1-s} f(k) \end{cases} \quad (2)$$

included among these,

$$\begin{cases} f(k) = \begin{cases} k(2-k), k < 1 \\ 1, k \geq 1 \end{cases} \\ k = (1-s) \frac{1}{2\sqrt{C_x^2 s^2 + C_y^2 \tan^2 \alpha}} \end{cases} \quad (3)$$

Where F_{zij} is the vertical load of four wheels; C_{xij} 、 C_{yij} are the longitudinal stiffness and lateral stiffness of each tyre, respectively; s is the longitudinal slip rate; μ is the road adhesion coefficient; k is the characteristic parameter due to the nonlinear change of tyre force caused by tyre slip, $k \geq 1$ denotes the linear interval of the tyre, $k < 1$ denotes the tyre non-linear interval. F_{xij}^* 、 F_{yij}^* denote the longitudinal and lateral normalized tyre forces of the 4 wheels. From equation (4), it can be seen that F_{xij}^* 、 F_{yij}^* are not correlated with the changes in the road adhesion coefficient.

The calculation of the normalized force becomes the key to estimating the road adhesion coefficient. In this paper, the vehicle state measured or estimated by known sensors is used as input to calculate the normalized force, thus laying the foundation for the design of the parameter estimator based on Equations (3) and (4).

The following equations describing the dynamics of the four-degree-of-freedom vehicle model can be obtained

$$\begin{cases} F_{z11,z12} = \left(\frac{1}{2} mg \pm m \frac{a_y h}{T_f} \right) \frac{b}{l} - \frac{1}{2} ma_x \frac{h}{l} \\ F_{z21,z22} = \left(\frac{1}{2} mg \pm m \frac{a_y h}{T_r} \right) \frac{a}{l} + \frac{1}{2} ma_x \frac{h}{l} \end{cases} \quad (5)$$

$$\begin{cases} \alpha_{1,12} = \alpha - \arctan\left(\frac{v_y + ar}{v_x \pm T_f r / 2} \right) \\ \alpha_{21,22} = \arctan\left(\frac{-v_y + br}{v_x \pm T_r r / 2} \right) \end{cases} \quad (6)$$

$$\lambda_{ij} = \frac{\omega_y r - v_{ij}}{v_{ij}} \quad (7)$$

Do tyre normalized processing of equation (2):

$$\begin{cases} v_{11,12} = v_{cog} + r \left(\pm \frac{T_f}{2} - a\beta \right) \\ v_{21,22} = v_{cog} + r \left(\pm \frac{T_f}{2} + b\beta \right) \end{cases} \quad (8)$$

$$\beta = \arctan\left(\frac{v_y}{v_x}\right) \quad (9)$$

$$v_{cog} = \sqrt{v_x^2 + v_y^2} \quad (10)$$

where h is the height of the vehicle body, α_{ij} is the tyre side deflection angle, ω_{ij} is the wheel angular velocity, r is the wheel radius, v_{cog} is the vehicle center velocity, and β is the center of mass side deflection angle.

For the calculation of the state variables in the longitudinal and lateral normalized forces F_{xij}^* , F_{yij}^* the reference equation. At this point, the three-degree-of-freedom vehicle model and the tyre model are established.

3. Design of Volumetric Kalman Filter Estimation Algorithm

3.1. Estimator Design

According to equations (1) and (4), a mathematical relationship between the road adhesion coefficient and the vehicle dynamics equations can be seen. In this paper, this relationship is be used to estimate the road adhesion coefficient using UKF.

Since most of the studies set the road attachment coefficient as a constant, it is usually assumed that μ takes a value between 0.1 and 1. Definition: system state variable $x = (\mu_{11}, \mu_{12}, \mu_{21}, \mu_{22})^T$, systematic observation variable $z = (a_x, a_y, \dot{\omega})^T$, input variable $\mu = (\alpha, F_{xij}^*, F_{yij}^*)^T$. $w(t)$, $v(t)$ is the process white noise and measurement white noise. Where μ_{11} , μ_{12} , μ_{21} , μ_{22} are the adhesion coefficients between the four tyres and the ground, and α is the front wheel turning angle.

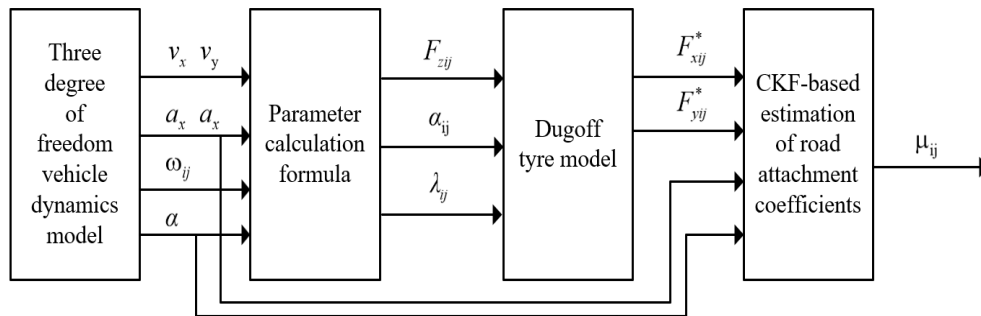


Figure 2. Schematic diagram of CKF based pavement adhesion coefficient estimation algorithm

3.2. Classical Kalman Filter

Classical Kalman filter theory is a filter theory applied to linear systems. Many physical processes, such as changes in room temperature, free-fall, the movement of satellites in orbit around the earth, and the GPS navigation of ships, can be approximated as a linear system. Consider the following state space expression to describe a linear system.

$$\text{Equation of state: } x(k) = Ax(k-1) + Bu(k) + w(k-1)$$

Set up the equation of state as:

$$x(t+1) = f[x(t), \mu(t) + w(t)] = \begin{bmatrix} 1 & 0 & 0 & 0 \\ 0 & 1 & 0 & 0 \\ 0 & 0 & 1 & 0 \\ 0 & 0 & 0 & 1 \end{bmatrix} \begin{bmatrix} \mu_{11} \\ \mu_{12} \\ \mu_{21} \\ \mu_{22} \end{bmatrix} + w(t) \quad (11)$$

The observation equation is:

$$z(t) = h[x(t), \mu(t) + v(t)] = \begin{bmatrix} \frac{F_{x11}^* \cos \alpha - F_{y11}^* \sin \alpha}{m} & \frac{F_{x12}^* \cos \alpha - F_{y12}^* \sin \alpha}{m} & \frac{F_{x21}^*}{m} & \frac{F_{x22}^*}{m} \\ \frac{F_{x11}^* \sin \alpha + F_{y11}^* \cos \alpha}{m} & \frac{F_{x12}^* \sin \alpha + F_{y12}^* \cos \alpha}{m} & \frac{F_{y21}^*}{m} & \frac{F_{y22}^*}{m} \\ J(3,1) & J(3,2) & J(3,3) & J(3,4) \end{bmatrix} \begin{bmatrix} \mu_{11} \\ \mu_{12} \\ \mu_{21} \\ \mu_{22} \end{bmatrix} + v(t) \quad (12)$$

Among them:

$$J(3,1) = \frac{a(F_{x11}^* \sin \alpha + F_{y11}^* \cos \alpha) - T_f(F_{x11}^* \cos \alpha - F_{y11}^* \sin \alpha)/2}{I_z}$$

$$J(3,2) = \frac{a(F_{x12}^* \sin \alpha + F_{y12}^* \cos \alpha) + T_f(F_{y12}^* \sin \alpha - F_{x12}^* \cos \alpha)/2}{I_z}$$

$$J(3,3) = \frac{T_f F_{x21}^* - b F_{y21}^*}{I_z}; \quad J(3,4) = \frac{T_f F_{x22}^* - b F_{y22}^*}{I_z}$$

The measurement noise covariance matrix

$$R = \begin{bmatrix} 1 & 0 & 0 & 0 \\ 0 & 1 & 0 & 0 \\ 0 & 0 & 1 & 0 \\ 0 & 0 & 0 & 1 \end{bmatrix}, \text{ the system noise covariance matrix}$$

$Q = I_{4 \times 4} * 0.1$, the system state variable

$x(0) = [1 \ 1 \ 1 \ 1]^T$, and the initial value of the error covariance matrix is $P(0) = I_{4 \times 4}$.

The normalized forces are calculated using the Dugoff tyre model. The inputs to the model are: front wheel angle of rotation, wheel speeds of all four wheels; longitudinal and lateral acceleration; lateral deflection angle of the center of mass; transverse angular velocity and longitudinal vehicle speed. The final normalized tyre force is obtained for all four wheels (Including vertical and lateral total of 8), as input to the CKF parameter estimator. The following figure shows the schematic diagram of the CKF based pavement adhesion coefficient estimation algorithm as shown in Fig2.

$$\text{Observation equation: } y(k) = Hx(k) + v(k)$$

Where, k discrete time, the state of the system at moment k ; $u(k)$ is the control input to the system, $y(k)$ is the observed signal to the state. $w(k)$ is the input white noise, also known as process noise, and $v(k)$ is the observation noise. A is the state transfer matrix, B is the noise distribution matrix, and H is the observation matrix.

$w(k)$ and $v(k)$ are white noises with zero mean. And,

they are independent of each other. Thus the following equation can be obtained.

$$\begin{cases} Ew(k) = 0 \\ Ev(k) = 0 \\ E(w(k)v^T(j)) = 0, \forall k, j \end{cases} \quad (13)$$

The matrices Q and R are the variance arrays corresponding to two noises which satisfy:

$$\begin{cases} E(w(k)w^T(j)) = Q\delta_{kj} \\ E(v(k)v^T(j)) = R\delta_{kj} \end{cases} \quad (14)$$

Where, $Q\delta_{kj} = 0, k \neq j$, $R\delta_{kj}$ takes any positive real number, depending on the actual equation.

The system gives the exact procedure of Kalman filtering:
State prediction equations:

$$\hat{x}(k) = Ax(k-1) + Bu(k) + w(k-1) \quad (15)$$

Error covariance prediction equation:

$$\hat{P}(k) = AP(k-1)A^T + Q \quad (16)$$

Gain equations:

$$K(k) = \hat{P}(k)H^T (H\hat{P}(k)H^T + R)^{-1} \quad (17)$$

Filtering equations

$$x(k) = \hat{x}(k) + K(k)(y(k) - H\hat{x}(k)) \quad (18)$$

Error covariance update equation:

$$P(k) = (1 - K(k)H)\hat{P}(k) \quad (19)$$

A total of five formulas that the five core formulas of the classical Kalman filter, the above classical Kalman filter is introduced.

3.3. Volumetric Kalman Filter

CKF transforms the nonlinear filtering problem into a problem of solving the product of a nonlinear function and a Gaussian probability density function, using the principle of volumetric numerical integration to approximate the state posterior distribution. The algorithm is highly accurate and stable[7]. And with the increase of the dimension of the system, the stability and accuracy of CKF will be more than UKF[8], at the same time, the computational amount of CKF is smaller than UKF, in view of the advantages of CKF, this paper selects CKF for the soft measurement of road adhesion coefficient.

The design of CKF is based on Bayesian filtering principle. According to the third-order spherical-Radial law, when the variable x obeys the normal distribution, it can be obtained as follows.

$$I_N(f) = \int_{R^n} f(x)N(x; \mu, P)dx \approx \sum_{i=1}^{2n} \omega_i f(\mu + \sqrt{P}\xi_i) \quad (20)$$

The covariance matrix P satisfies $\sqrt{P}\sqrt{P}^T = P$;

$$\omega_i = 1/2n ; \quad \xi_i = \sqrt{n}[\varepsilon]_i ; \quad [\varepsilon]_i \in \begin{bmatrix} \begin{pmatrix} 1 \\ 0 \\ c \\ 0 \end{pmatrix} & \begin{pmatrix} 0 \\ 0 \\ c \\ 1 \end{pmatrix} & \begin{pmatrix} -1 \\ 0 \\ c \\ 0 \end{pmatrix} & \begin{pmatrix} 0 \\ 0 \\ c \\ -1 \end{pmatrix} \end{bmatrix}$$

The core idea of CKF's algorithm is to implement the nonlinear estimation of 2n equally weighted volume points calculated by the Spherical-Radial volume rule. The algorithmic processing flow of CKF filtering is as follows:

Based on the estimate-and discrepancy moment k-1, the volume point initialisation is calculated using equation (20) to generate the volume point:

$$\begin{cases} S(k-1) = \text{chol}\{P(k-1)\} \\ \hat{X}_i(k-1) = S(k-1)\xi_i + X(k-1) \end{cases} \quad (21)$$

Nonlinear Propagation of Volume Points:

$$X_i^*(k-1) = f(\hat{X}_i(k-1), U(k)) \quad (22)$$

$$\text{Status prediction: } \hat{X}(k) = \sum_{i=1}^{2n} \omega_i X_i^*(k-1) \quad (23)$$

forecast variance:

$$\hat{P}(k) = \sum_{i=1}^{2n} \omega_i X_i^*(k-1)X_i^*(k-1)^T - \hat{X}(k)\hat{X}(k)^T + Q \quad (24)$$

Calculate the volume point based on the estimate and variance at moment k:

$$\hat{S}(k) = \text{chol}\{\hat{P}(k)\} \quad (25)$$

$$\hat{X}_i(k) = \hat{S}(k)\xi_i + \hat{X}(k) \quad (26)$$

Calculation of volumetric point values after propagation of the observation equation:

$$Y_i^*(k) = h(\hat{X}_i(k), U(k)) \quad (27)$$

$$\text{Observations forecast: } \hat{Y}(k) = \sum_{i=1}^m \omega_i Y_i^*(k) \quad (28)$$

Estimating the new observation covariance:

$$P_{yy}(k) = \sum_{i=1}^m \omega_i Y_i^*(k)Y_i^*(k)^T - y(k)y(k)^T + R \quad (29)$$

Estimating the covariance:

$$P_{xy}(k) = \sum_{i=1}^m \omega_i \hat{X}_i(k)Y_i^*(k)^T - \hat{X}(k)\hat{Y}(k)^T \quad (30)$$

Calculating Kalman Gain:

$$K(k) = P_{xy}(k)P_{yy}^{-1}(k) \quad (31)$$

Status Update:

$$X(k) = \hat{X}(k) + K(k)(Y(k) - \hat{Y}(k)) \quad (32)$$

Estimated covariance values:

$$P(k) = \hat{P}(k) + K(k)P_{yy}(k)K(k)^T \quad (33)$$

At this point, the CKF algorithm process ends, and the CKF will recursively push in real time to the next point of the calculation of the iterative loop has reached the final result.

4. Simulation Analysis of Road Attachment Coefficient Estimation

This paper addresses the design of soft measurement of road adhesion coefficient, while Carsim simulation software has a wealth of vehicle dynamics models, including the body, tyres, braking system and transmission system. Vehicle dynamics model, including the body, tyres, braking system, driveline system and other subsystems, the model precision is high, and its simulation test application has a strong practical application. Its simulation test application has strong practical application value. Therefore, this paper adopts the joint simulation test of Carsim and simulink, and selects the sdan E-class car as the simulation vehicle in this paper, and some of its parameters are shown in the table:

Table 1. The part parameters of the vehicle table

Vehicle parameter	Symbol	Numerical value	Unit
Overall vehicle mass	M	1650	kg
Wheel base	D	3050	mm
Center of gravity height	H	530	mm
Effective radius of tires	S	353	mm
Vehicle length	L	4868	mm

After setting three different road conditions with different road adhesion coefficients in Carsim, the filtered estimates of the road adhesion coefficients were compared with the actual values as a way to verify that the algorithm proposed in this paper is effective. The model is simulated, and the relationship between the estimated and given values of the road simulation coefficients is obtained as shown in Fig. 3. From the simulation results, it can be obtained that the road adhesion coefficients of all four wheels converge to the real

values in a short time. The details are as follows:

Setting the road adhesion coefficient at 0.9 corresponds to a dry concrete road surface, and the vehicle simulation condition is: driving at an initial speed of 60 km/h, the simulation results using the UKF algorithm are shown in Fig. 3. Under the high road adhesion coefficient of 0.9, the estimated value stabilizes to the set value of 0.9 in about 15s, and converges to 0.88-0.92 after 15s.

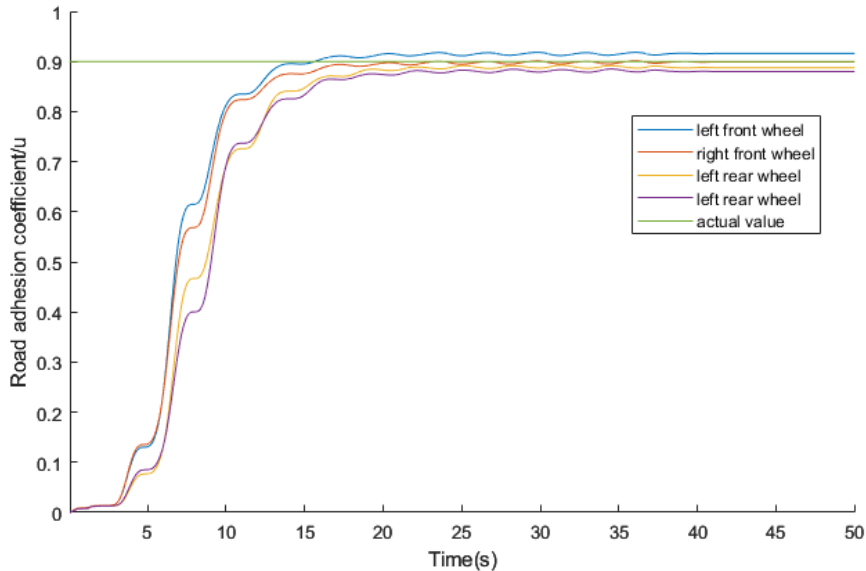


Figure 3. Simulation of high adhesion coefficient pavement

Setting the road adhesion coefficient to 0.6 corresponds to the wet concrete road surface, the vehicle simulation condition is: driving at an initial speed of 60 km/h, the simulation results using the UKF algorithm are shown in Fig.

4. In the case of the set medium road adhesion coefficient of 0.6, the estimated value stabilizes to the set value of 0.6 in about 10s, and converges to 0.57-0.62 after 10s.

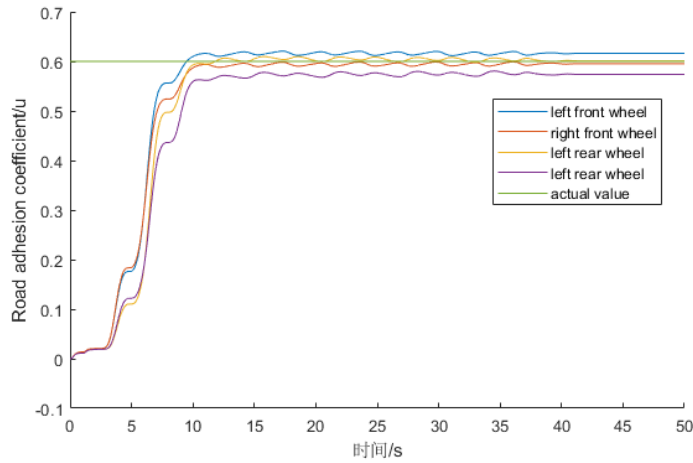


Figure 4. Simulation of middle adhesion coefficient pavement

Setting the road adhesion coefficient to 0.3 corresponds to the rainy road surface, and the simulation condition of the vehicle is: driving at an initial speed of 60 km/h, the simulation results using the UKF algorithm are shown in Fig.

5. With the low road adhesion coefficient of 0.3, the estimated value stabilise to the set value of 0.3 in about 7s and converges to 0.29-0.31 after 7s.

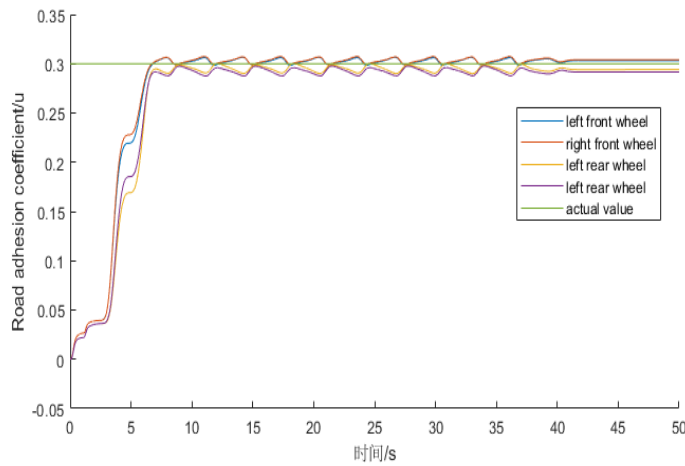


Figure 5. Simulation of low adhesion coefficient pavement

The overall convergence of per-wheel recognition is slightly slower for medium and high road adhesion coefficients compared to low road adhesion coefficients, which is in line with the actual driving conditions[9]. This shows the effectiveness of applying the UKF filter estimator in this paper for the estimation of road adhesion coefficients for different road surfaces.

5. Conclusion

The paper establishes a three-degree-of-freedom vehicle estimation model using Dugoff tyre model, and designs a road adhesion estimation algorithm based on the theory of volumetric Kalman filtering, the estimation value stabilizes to the set value of 0.9 around 15s, and then converges to 0.88-0.92 after 15s, and stabilizes to the set value of 0.6 around 10s, and converges to 0.57-0.62 after 10s. 0.57-0.62, stabilized to the set value of 0.3 in about 7s, and converged to 0.29-0.31 after 7s. Calculations show that the estimation error of the estimation algorithm based on the Volumetric Kalman Filter is less than 5%, which proves that the algorithm is accurate and consistent with the real-time estimation. It is proved that the algorithm can complete the initial design well in terms of both accuracy and real-time performance to achieve the purpose of soft measurement of road adhesion coefficient.

Acknowledgment

This paper was supported by the funds. The funds are as follows: Tianjin graduate student Scientific research and innovation projects (2022SKYZ380); Tianjin graduate student Scientific research and innovation projects (2022SKYZ388).

References

- [1] Yu Zhuo-Ping, Zuo Jian-Ling and Zhang Li-Jun, "A Review of the Development Status of Pavement Adhesion Coefficient Estimation Technology", *Automotive Engineering*, Vol. 6, pp.
- [2] Yanliang Pei, "Estimation of road surface adhesion coefficient for active safety system of electric vehicle", Master, Shenyang University of Technology, 2013. Available on: 16 October 2023.
- [3] M. Morii, H. Yasuo, T. Kashihara, T. Iwamoto, and M. Sugimoto, "Pavement Condition Detector Using a High Peak Power Fibre Laser," *IEEE Transactions on Industry Applications*, vol. 120, pp.
- [4] Wang Hesen, "Research on Longitudinal Safety Control Strategy for Cargo Vehicles Based on the Estimation of Road

- Surface Adhesion Coefficient", M.S., Shijiazhuang Railway University, 2020.000191.
- [5] Jinxi Chen, "Research on Algorithm of Pavement Adhesion Coefficient Estimation Based on Volumetric Kalman Filtering", Master's Degree, University of Electronic Science and Technology, 17 April 2023.
- [6] G. Li, R.C. Xie, S.Y. Wei and C.F. Zong, "Estimation of vehicle state and road surface adhesion coefficient based on two-volume Kalman filtering", *Science in China: Technological Sciences*, vol. 45, no. 4, pp. 403-414, 2015.
- [7] C. Fernandez-Prades and J. Vila-Valls, Bayesian Nonlinear Filtering Using Orthogonal and Cubic Rules Applied to Positioning Sensor Data Fusion, 2010 IEEE International Conference on Communications, Cape Town, South Africa: May 2010, pp. 1-5.
- [8] Li Jun Tang, "Research on Cubature Kalman Filter and its Application in Navigation", PhD, Harbin Engineering University, 2012. Available on: 16 October 2023.
- [9] Hou-Long Li, "Research and Simulation on Control Strategy of Automatic Emergency Braking System Based on Driving Characteristics and Road Surface Adhesion Coefficient", M.S., Chang'an University, China, 2021.